



# The phase structure and electric properties of low-temperature sintered (K, Na)NbO<sub>3</sub>-based piezoceramics modified by CuO

Jia-Jun Zhou<sup>a</sup>, Li-Qian Cheng<sup>b</sup>, Ke Wang<sup>b,\*</sup>, Xiao-Wen Zhang<sup>b</sup>, Jing-Feng Li<sup>b</sup>, Hong Liu<sup>a</sup>,  
Jing-Zhong Fang<sup>a</sup>

<sup>a</sup>Institute of Optics and Electronics, Chinese Academy of Sciences, Chengdu 610209, China

<sup>b</sup>State Key Laboratory of New Ceramics and Fine Processing, School of Materials Science and Engineering, Tsinghua University, Beijing 100084, China

Received 30 August 2013; received in revised form 17 September 2013; accepted 4 October 2013

Available online 10 October 2013

## Abstract

0.25 wt% CuO-doped (Li,K,Na)(Nb,Ta)O<sub>3</sub>-AgSbO<sub>3</sub> lead-free piezoceramics with pure perovskite structure were successfully prepared at a sintering temperature below 1000 °C. The sintering temperature of KNN-based piezoceramics was effectively reduced by about 100 °C due to the enhanced densification process induced by the addition of CuO. Besides, the acceptable sintering temperature window was broadened by the addition of CuO. It is found that the CuO-doped samples show slightly higher tetragonal–orthorhombic phase transition point ( $T_{T-O}$ ) but a lower Curie point ( $T_c$ ), compared to undoped ones. The KNN-based piezoceramics became “hard” as CuO was added, supported by an increase of  $Q_m$ . Fairly good electrical properties of  $d_{33}^* = 383$  pm/V,  $\epsilon_r = 860$ ,  $Q_m = 188$  and  $T_c = 215$  °C could be obtained in dense CuO-modified KNN-based piezoceramics sintered at 970 °C, demonstrating promising potential in practical applications.

© 2013 Elsevier Ltd and Techna Group S.r.l. All rights reserved.

**Keywords:** C. Piezoelectric properties; D. Perovskites; D. Niobates; Lead-free

## 1. Introduction

Traditional lead-based piezoceramics have been widely used in sensors, transducers, actuators, and other important devices for decades. As an increasing concern of the toxicity of lead in traditional Pb(Zr,Ti)O<sub>3</sub>-based piezoceramics, lead-free piezoceramics have drawn much attention recently [1–3]. Among various kinds of lead-free piezoceramics systems, (K,Na)NbO<sub>3</sub> (KNN)-based ceramics show relatively high Curie point as well as attractive piezoelectric activity comparable to PZT-based ceramics; therefore, they are considered as one of the most promising lead-free candidates for the substitution of PZT-based ceramics [4–8].

KNN-based piezoceramics fabricated by conventional methods are normally sintered at high temperatures above 1000 °C, resulting in several problems. Firstly, the inevitable volatilization of alkaline elements during high temperature firing leads to compositional deviation, which greatly increases the difficulty in reproducibility

of sample preparation, since the amount of alkaline elements has a significant influence on the phase structure as well as electrical properties [9,10]. Secondly, the high sintering temperature is very close to the liquid–solid phase transition line of this system, easily leading to compositional segregation and abnormal grain growth [11,12]. Thirdly, for applications in multilayer-structured devices, low-temperature sintering of the piezoceramics will reduce the cost significantly, since the expensive Ag–Pd inner electrode normally used for high temperature sintering (above 1000 °C) can be replaced by inexpensive electrode materials such as copper [13]. Therefore, it is of great necessity to develop the low temperature sintering technology for KNN-based piezoceramics.

In our previous work, excellent piezoelectric performance with  $d_{33}^* = 598$  pm/V ( $E_{max} = 1$  kV/mm) was obtained in 0.95Li<sub>0.02</sub>(Na<sub>0.53</sub>K<sub>0.48</sub>)<sub>0.98</sub>Nb<sub>0.8</sub>Ta<sub>0.2</sub>O<sub>3</sub>-0.05AgSbO<sub>3</sub> (LKNNTAS) lead-free piezoceramics, which will serve as the base material in the present work [14]. On the other hand, CuO has been proved as an effective sintering aid for many kinds of piezoceramics. But it is also reported that the addition of a large amount of CuO will induce undesirable secondary phases, which deteriorates piezoelectric properties [15–17]. According to the above considerations, proper

\*Corresponding author. Tel.: +86 10 62784845; fax: +86 10 62771160.

E-mail address: [wang-ke@tsinghua.edu.cn](mailto:wang-ke@tsinghua.edu.cn) (K. Wang).

amount of CuO (0.25 wt%) was selected to lower the sintering temperature of LKNNTAS piezoceramics without the introduction of secondary phase. The phase structure and electrical properties of CuO-modified LKNNTAS piezoceramics were systematically studied in the present work.

## 2. Experimental procedure

KNN-based lead-free piezoceramics exhibiting high piezoelectric performance with the composition of  $0.95\text{Li}_{0.02}(\text{Na}_{0.53}\text{K}_{0.48})_{0.98}\text{Nb}_{0.8}\text{Ta}_{0.2}\text{O}_3-0.05\text{AgSbO}_3$  were prepared by the solid-state reaction method, according to the Ref. [14]. Then, 0.25 wt% of CuO was added to previously synthesized LKNNTAS powders (abbreviated as LKNNTAS–CuO) by ball milling for 24 h in ethanol using  $\text{ZrO}_2$  balls. After the slurry was dried, the mixed powders were pressed into small disks of 10 mm in diameter, followed by a cold isostatic pressing at 200 MPa. The sintering temperature was optimized according to the shrinkage curves.

The shrinkage curves of LKNNTAS and LKNNTAS–CuO piezoceramics were measured by a dilatometer (Netzsch DIL 402 PC, Germany) at a heating rate of  $5^\circ\text{C}/\text{min}$ . The crystal structure of the sintered samples was determined by X-ray diffraction (XRD) characterization with monochromatic  $\text{Cu K}\alpha_1$  radiation (Rigaku, D/Max 2500, Tokyo, Japan). The as-sintered sample surfaces were observed by field emission scanning electron microscopy (FESEM, S-7001F, JEOL, Japan). The piezoelectric properties were determined by the strain–field method, using the piezo-testing system (aixACCT TF Analyzer 1000, Germany). The converse piezoelectric constant  $d_{33}^*$  was calculated as  $S_{\text{max}}/E_{\text{max}}$ . Evaluation of dielectric temperature stability was measured at 1 kHz in a temperature-regulated chamber, which was connected with Agilent 4194 (Hewlett-Packard, Palo Alto, CA, USA) at 1 kHz.

## 3. Results and discussion

Fig. 1 shows the shrinkage and shrinkage rate curves of LKNNTAS and LKNNTAS–CuO piezoceramics, respectively. The LKNNTAS sample shows the peak shrinkage rate around

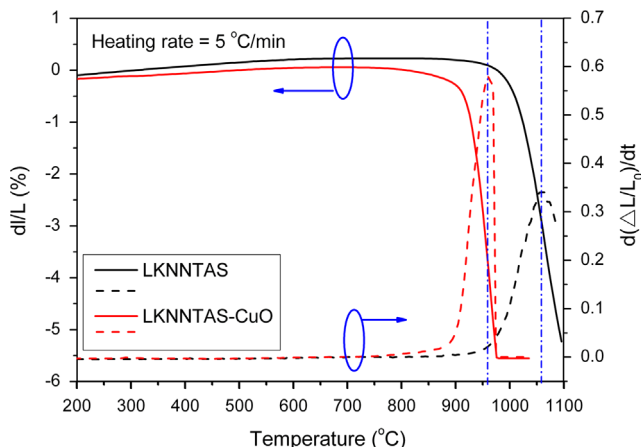


Fig. 1. The shrinkage and shrinkage rate curves of LKNNTAS and LKNNTAS–CuO piezoceramics, respectively.

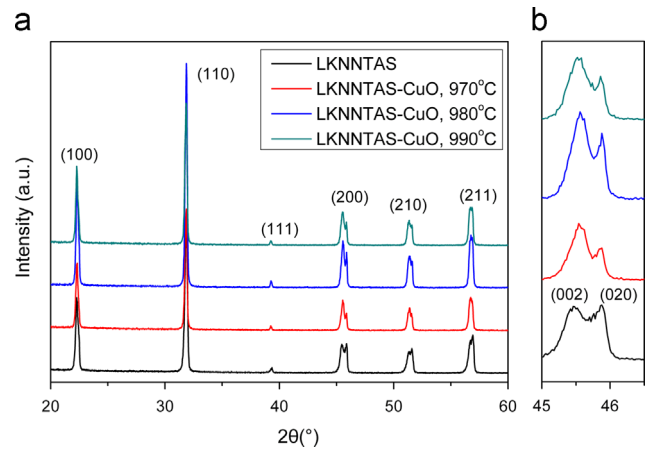


Fig. 2. XRD patterns of LKNNTAS and LKNNTAS–CuO piezoceramics.

$1060^\circ\text{C}$  and the optimal sintering temperature for the ceramics is about  $1080^\circ\text{C}$  with a holding time of 2 h. With the addition of CuO, the temperature corresponding to the peak shrinkage rate is significantly reduced to about  $960^\circ\text{C}$ . It can be speculated that the liquid phases is formed below  $900^\circ\text{C}$ , ruling out the possibility of CuO itself as the liquid phase (the melting point of CuO is  $1326^\circ\text{C}$ ). The sintering temperature for LKNNTAS–CuO was selected in the range of  $970\text{--}990^\circ\text{C}$ .

Fig. 2 shows the XRD patterns of LKNNTAS and CuO-modified LKNNTAS ceramics sintered at different temperatures in the  $2\theta$  range from  $20^\circ$  to  $60^\circ$ . All the compositions demonstrate pure perovskite phases, and no trace of second phase is found due to the reasonable content of CuO. This result indicates that a small amount of  $\text{Cu}^{2+}$  may incorporate into the lattice of KNN matrix. The relative intensity of (002)/(020) peaks around  $2\theta=45^\circ$  changes obviously, according to the enlarged area in Fig. 2(b). It is well known that KNN-based piezoceramics usually show orthorhombic and/or tetragonal symmetry at room temperature, which can be identified by the following details in the XRD patterns [18]. When the material is of orthorhombic phase with cell parameters  $a \approx c > b$ ,  $I_{(002)}/I_{(020)}$  roughly equals 2 and the (002) peak appears at a smaller Bragg angle, but the  $I_{(002)}/I_{(020)}$  decreases to 0.5 for a tetragonal phase with  $a=b < c$  [19,20]. In the present study, the  $I_{(002)}/I_{(020)}$  of LKNNTAS piezoceramics is about 1, indicating the coexistence of orthorhombic and tetragonal phases in LKNNTAS samples. With the addition of CuO, the  $I_{(002)}/I_{(020)}$  increases, implying that orthorhombic phase becomes dominant in LKNNTAS–CuO ceramics. It is thus concluded that the addition of 0.25 wt% CuO favors the phase transformation from tetragonal to orthorhombic in LKNNTAS lead-free piezoceramics at room temperature. It is also observed that the differences in the investigated sintering temperature range have little influence on the phase structure of LKNNTAS–CuO ceramics which is probable due to the suppressed violation of alkali elements at the low temperature sintering.

Fig. 3 shows the SEM images of the as-sintered surfaces of LKNNTAS and LKNNTAS–CuO piezoceramics. Pure LKNNTAS ceramics sintered at  $1080^\circ\text{C}$  show a relatively

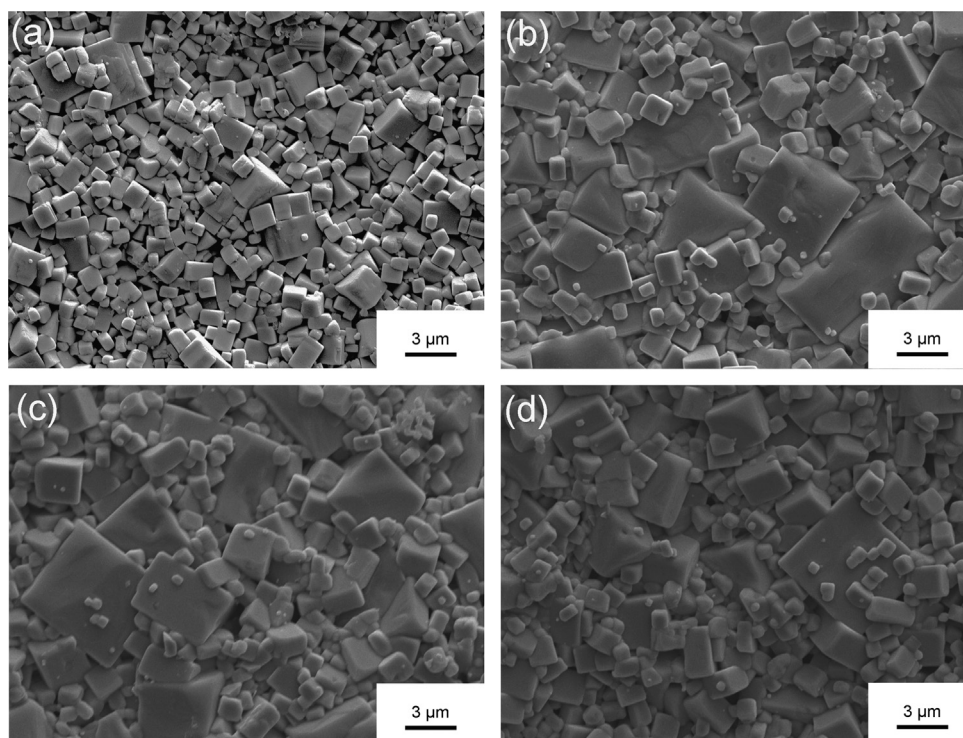


Fig. 3. SEM images of the as-sintered surfaces of LKNNTAS and LKNNTAS–CuO piezoceramics, (a) LKNNTAS, (b) LKNNTAS–CuO sintered at 970 °C, (c) LKNNTAS–CuO sintered at 980 °C, (d) LKNNTAS–CuO sintered at 990 °C.

uniform distribution of grain size, with some larger grains of 2–3  $\mu\text{m}$  and smaller grains of 1  $\mu\text{m}$ . The average grain size of LKNNTAS increases with the addition of CuO, which is possibly attributed to the appearance of liquid phases during the sintering process. However, the addition of CuO strengthens the bimodal distribution of grain size. For LKNNTAS–CuO ceramics sintered at 970 °C, it is observed that large grains up to 4–5  $\mu\text{m}$  and small grains of 1  $\mu\text{m}$  coexist. This phenomenon is probable a consequence of the inhomogeneous distribution of liquid phase, while the liquid phases only promote growth of local grains [21]. Meanwhile, there is a tendency that the average grain size of LKNNTAS–CuO piezoceramics decreases as the sintering temperature increases, which implies that the distribution of liquid phases becomes more homogeneous as the sintering temperature increases.

Fig. 4 shows the temperature dependence of the relative dielectric constant of CuO doped and undoped LKNNTAS piezoceramics measured at 1 kHz during the heating process (2 °C/min). Considering the similar phase structures of LKNNTAS–CuO piezoceramics sintered at different temperatures, only the sample sintered at 970 °C was provided here. Both the LKNNTAS and LKNNTAS–CuO ceramics undergo orthorhombic–tetragonal phase transition ( $T_{T-O}$ ) and tetragonal–cubic phase transition ( $T_c$ ) during the measured temperature range. The pure LKNNTAS ceramics possess  $T_c$  and  $T_{T-O}$  of 235 °C and 30 °C, respectively. With the addition of CuO, the  $T_c$  of LKNNTAS slightly decreases to 215 °C, while the  $T_{T-O}$  increases to 60 °C. The increased  $T_{T-O}$  of LKNNTAS–CuO piezoceramics indicates that the orthorhombic phase is dominant at room temperature, in consistent with the

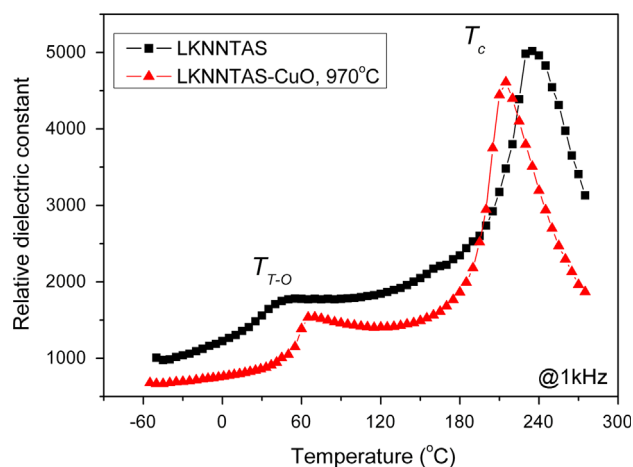


Fig. 4. Temperature dependence of the relative dielectric constant of LKNNTAS and LKNNTAS–CuO (sintered at 970 °C) piezoceramics.

analysis of XRD patterns. The dielectric properties of LKNNTAS piezoceramics decrease with the addition of CuO, showing similar tendency to the previous work [15–17].

Fig. 5 shows the representative  $P$ – $E$  loops of LKNNTAS and LKNNTAS–CuO piezoceramics measured at a frequency of 1 Hz. Well-saturated hysteresis loops are obtained for all the compositions. LKNNTAS piezoceramics possess the  $P_r$  and  $E_c$  of 14.2  $\mu\text{C}/\text{cm}^2$  and 7.8 kV/cm, respectively. The LKNNTAS–CuO piezoceramics sintered at 970 °C and 980 °C nearly have the same ferroelectric properties, that coercive fields  $E_c$  are 6.1 kV/cm for both samples, while the remnant polarizations

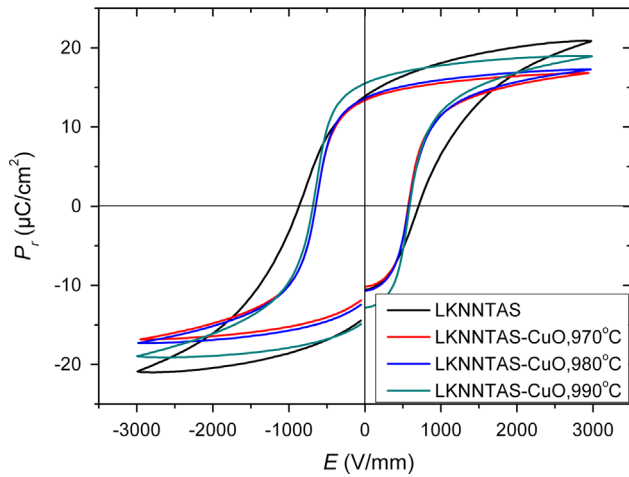


Fig. 5.  $P$ - $E$  loops of LKNNTAS and LKNNTAS-CuO piezoceramics.

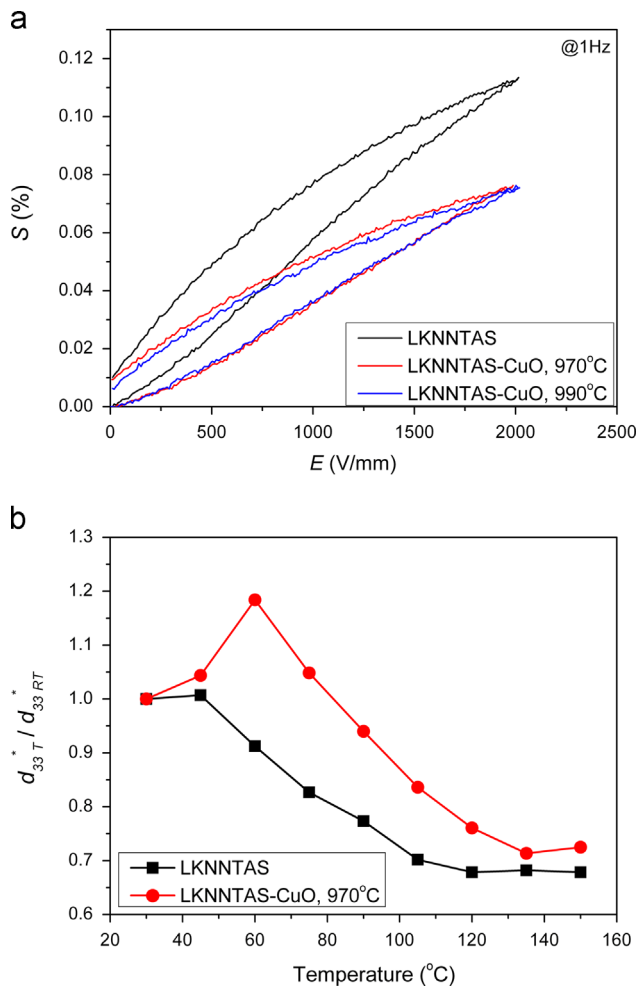


Fig. 6. Room-temperature  $S$ - $E$  curves (a), and temperature dependent  $d_{33}^*/d_{33RT}^*$  (b) of LKNNTAS and LKNNTAS-CuO piezoceramics.

$P_r$  are  $12.6 \mu\text{C}/\text{cm}^2$  and  $13.0 \mu\text{C}/\text{cm}^2$ , respectively. The LKNNTAS-CuO piezoceramics sintered at  $990^\circ\text{C}$  possess slightly higher  $E_c$  of  $6.4 \text{ kV}/\text{cm}$  and  $P_r$  of  $15.2 \mu\text{C}/\text{cm}^2$  than the other two samples. The  $E_c$  of LKNNTAS piezoceramics

decreases obviously with the addition of CuO, which seems to be contradictory with the increase of  $Q_m$ . Similar results have also been found in CuO-doped KNN-based piezoceramics in previous reports [22,23], which can be attributed to the complex substitution of  $\text{Cu}^{2+}$  to A/B-sites in KNN matrix.

Fig. 6 shows the representative  $S$ - $E$  curves and temperature dependence of  $d_{33T}^*/d_{33RT}^*$  of LKNNTAS and LKNNTAS-CuO piezoceramics. The converse piezoelectric constant  $d_{33}^*$  was calculated from  $S$ - $E$  curves. All the compositions show typical linear  $S$ - $E$  curves of ferroelectric ceramics. With the addition of CuO, the field-induced strains of LKNNTAS piezoceramics decreases from 0.11% to 0.076% under the electric field of  $2 \text{ kV}/\text{mm}$  at room temperature, which is mainly attributed to the following two reasons. Firstly, the addition of 0.25 wt% CuO increases the  $T_{T-O}$  of LKNNTAS piezoceramics from room temperature to around  $60^\circ\text{C}$ , so the room-temperature piezoelectricity will decrease as a result of significantly weakened polymorphism phase transition (PPT). Secondly, the  $\text{Cu}^{2+}$  can act as an acceptor into KNN matrix and most likely occupies B-site ( $\text{Nb}^{5+}$ ), which leads to the “hardening” effect [21–23]. This behavior will lower the extrinsic contribution of strains under electric field. It should be noted that the LKNNTAS-CuO ceramics sintered at  $970^\circ\text{C}$  and  $990^\circ\text{C}$  almost have the same piezoelectric constant, demonstrating a broader sintering temperature window than the undoped samples. The  $d_{33}^*$  of LKNNTAS piezoceramics varies as the temperature changes and decreases  $\sim 32\%$  (from 560 to 380 pm/V) when the temperature increases from room temperature ( $30^\circ\text{C}$ ) to  $150^\circ\text{C}$ . However, the  $d_{33}^*$  of LKNNTAS-CuO piezoceramics firstly increases with the rising temperature and shows a peak value of 452 pm/V at  $60^\circ\text{C}$ , then decreases  $\sim 28\%$  at the temperature of  $150^\circ\text{C}$ . The peak value of  $d_{33}^*$  of LKNNTAS-CuO around  $T_{T-O}$  ( $60^\circ\text{C}$ ) is mainly attributed by the PPT effect in which polarization switching will become easier under the same electric field.

Table 1 shows the room-temperature electrical properties of LKNNTAS and LKNNTAS-CuO piezoceramics. The  $d_{33}^*$ ,  $k_p$  and  $\varepsilon_r$  of LKNNTAS piezoceramics decreases with the addition of CuO due to the combined influences of the significantly weakened PPT effect and the “hardening” effect. At the same time, LKNNTAS-CuO ceramics show higher  $Q_m$  and lower  $\tan \delta$  than the undoped LKNNTAS ceramics. Differences in sintering temperatures have little influence on the electrical properties of LKNNTAS-CuO ceramics, indicating that a broader sintering temperature window was achieved. Sintered at a low temperature of  $970^\circ\text{C}$ , the LKNNTAS-CuO sample shows the electrical properties of  $d_{33}^* \sim 383 \text{ pm}/\text{V}$ ,  $k_p \sim 33.3\%$ ,  $\varepsilon_r \sim 860$ , demonstrating fairly good piezoelectric performance in KNN-based piezoceramics [15–17,21].

#### 4. Conclusions

The phase structure and electrical properties of CuO-modified LKNNTAS piezoceramics sintered at a low temperature have been systematically investigated. Dense LKNNTAS sample with pure perovskite phase sintered below  $1000^\circ\text{C}$  was achieved by the addition of proper amount of CuO.

Table 1  
Electrical properties of LKNNTAS and LKNNTAS–CuO piezoceramics at room temperature.

| Composition | Sintering temperature (°C) | $d_{33}^*$ (pm/V) | $k_p$ (%) | $\epsilon_r$ (1 kHz) | $Q_m$ | $\tan \delta$ (%) (1 kHz) |
|-------------|----------------------------|-------------------|-----------|----------------------|-------|---------------------------|
| LKNNTAS     | 1080                       | 560               | 43        | 1560                 | 35    | 3.9                       |
| LKNNTAS–CuO | 970                        | 383               | 33.3      | 860                  | 188   | 0.8                       |
| LKNNTAS–CuO | 990                        | 377               | 33.8      | 980                  | 160   | 1.3                       |

The addition of CuO increases the  $T_{T-O}$  of LKNNTAS ceramics, while decreases its  $T_c$  slightly. The sintering temperature window becomes broader with the addition of CuO. A large increase of  $Q_m$  is induced by CuO-doping. LKNNTAS–CuO piezoceramics sintered at the temperature as low as 970 °C exhibit attractive electrical properties of  $d_{33}^* \sim 383$  pm/V,  $\epsilon_r \sim 860$ ,  $Q_m \sim 188$  and  $T_c \sim 215$  °C, demonstrating very promising potential in practical applications.

### Acknowledgments

This work was supported by National Nature Science Foundation of China (Grant nos. 51221291, 51211140345) and the Ministry of Science and Technology of China under the Grant 2009CB623304, as well as by State Key Laboratory of New Ceramics and Fine Processing Tsinghua University (KF201309).

### References

- [1] E. Cross, Lead-free at last, *Nature* 432 (2004) 24–25.
- [2] J. Rödel, W. Jo, K.T.P. Seifert, E.M. Anton, T. Granzow, D. Damjanovic, Perspective on the development of lead-free piezoceramics, *Journal of the American Ceramic Society* 92 (2009) 1153–1177.
- [3] T.R. Shrout, S.J. Zhang, Lead-free piezoelectric ceramics: alternatives for PZT?, *Journal of Electroceramics* 19 (2007) 111–124.
- [4] Y. Saito, H. Takao, T. Tani, T. Nonoyama, K. Takatori, T. Homma, T. Nagaya, M. Nakamura, Lead-free piezoceramics, *Nature* 432 (2004) 84–87.
- [5] E. Ringgaard, T. Wurlitzer, Lead-free piezoceramics based on alkali niobates, *Journal of the European Ceramic Society* 25 (2005) 2701–2706.
- [6] W. Jo, R. Dittmer, M. Acosta, J. Zang, C. Groh, E. Sapper, K. Wang, J. Rödel, Giant electric-field-induced strains in lead-free ceramics for actuator applications – status and perspective, *Journal of Electroceramics* 29 (2012) 71–93.
- [7] S. Wongsanmai, S. Ananta, R. Yimnirun, Effect of Li addition on phase formation behavior and electrical properties of  $(K_{0.5}Na_{0.5})NbO_3$  lead free ceramics, *Ceramics International* 38 (2012) 147–152.
- [8] P. Palei, M. Pattanaik, P. Kumar, Effect of oxygen sintering on the structural and electrical properties of KNN ceramics, *Ceramics International* 38 (2012) 851–854.
- [9] K. Wang, J.F. Li, (K, Na) $NbO_3$ -based lead-free piezoceramics: phase transition, sintering and property enhancement, *Journal of Advanced Ceramics* 1 (2012) 24–37.
- [10] S. Zhang, H.J. Lee, C. Ma, X. Tan, Sintering effect on microstructure and properties of (K,Na) $NbO_3$  ceramics, *Journal of the American Ceramic Society* 94 (2011) 3659–3665.
- [11] Y. Wang, D. Damjanovic, N. Klein, N. Setter, High-temperature instability of Li- and Ta-modified (K,Na) $NbO_3$  piezoceramics, *Journal of the American Ceramic Society* 91 (2008) 1962–1970.
- [12] J. Fang, X. Wang, R. Zuo, Z. Tian, C. Zhong, L. Li, Narrow sintering temperature window for (K, Na) $NbO_3$ -based lead-free piezoceramics caused by compositional segregation, *Physica Status Solidi A* 208 (2011) 791–794.
- [13] C.A. Randall, A. Kelnberger, G.Y. Yang, R.E. Eitel, T.R. Shrout, High strain piezoelectric multilayer actuators—A material science and engineering challenge, *Journal of Electroceramics* 14 (2005) 177–191.
- [14] J.J. Zhou, K. Wang, F. Li, J.F. Li, X.W. Zhang, Q.M. Wang, High and frequency-insensitive converse piezoelectric coefficient obtained in  $AgSbO_3$ -modified (Li, K, Na)(Nb,Ta) $O_3$  lead-free piezoceramics, *Journal of the American Ceramic Society* 92 (2013) 519–523.
- [15] H.Y. Park, J.Y. Choi, M.K. Choi, K.H. Cho, S. Nahm, H.G. Lee, H.W. Kang, Effect of CuO on the sintering temperature and piezoelectric properties of  $(Na_{0.5}K_{0.5})NbO_3$  lead-free piezoelectric ceramics, *Journal of the American Ceramic Society* 91 (2008) 2374–2377.
- [16] Z.Y. Shen, Y. Xu, J.F. Li, Enhancement of  $Q_m$  in CuO-doped compositionally optimized Li/Ta-modified (Na,K) $NbO_3$  lead-free piezoceramics, *Ceramics International* 38 (2012) S331–S334.
- [17] R. Huang, Y. Zhao, X. Zhang, Y. Zhao, R. Liu, H. Zhou, Low-temperature sintering of CuO-doped  $0.94(K_{0.48}Na_{0.535})NbO_3$ – $0.06LiNbO_3$  lead-free piezoelectric ceramics, *Journal of the American Ceramic Society* 93 (2010) 4018–4021.
- [18] Y. Guo, K. Kakimoto, H. Ohsato, Phase transitional behavior and piezoelectric properties of  $(Na_{0.5}K_{0.5})NbO_3$ – $LiNbO_3$  ceramics, *Applied Physics Letters* 85 (2004) 4121.
- [19] Y.J. Dai, X.W. Zhang, K.P. Chen, Morphotropic phase boundary and electrical properties of  $K_{1-x}Na_xNbO_3$  lead-free ceramics, *Applied Physics Letters* 94 (2009) 042905.
- [20] K. Wang, J.F. Li, Analysis of crystallographic evolution in (Na,K) $NbO_3$ -based lead-free piezoceramics by x-ray diffraction, *Applied Physics Letters* 91 (2007) 262902.
- [21] Y. Zhao, Y. Zhao, R. Huang, R. Liu, H. Zhou, Effect of sintering temperature on microstructure and electric properties of  $0.95(K_{0.5}Na_{0.5})NbO_3$ – $0.05Li(Nb_{0.5}Sb_{0.5})O_3$  with copper oxide sintering aid, *J. Am. Ceram. Soc.* 94 (2011) 656–659.
- [22] E. Li, H. Kakimoto, S. Wada, T. Tsurumi, Influence of CuO on the structure and piezoelectric properties of the alkaline niobate-based lead-free ceramics, *Journal of the American Ceramic Society* 90 (2007) 1787–1791.
- [23] N.M. Hagh, K. Kerman, B. Jadidian, A. Safari, Dielectric and piezoelectric properties of  $Cu^{2+}$ -doped alkali niobates, *Journal of the European Ceramic Society* 29 (2009) 2325–2332.